Ultrasound in Med. & Biol., Vol. 30, No. 2, pp. 205–214, 2004

0301-5629/04/$–see front matter

ELSEVIER

doi:10.1016/j.ultrasmedbio.2003.10.006

● *Original Contribution*

EFFECTS OF AGGREGATION OF RED CELLS AND LINEAR VELOCITY GRADIENTS ON THE CORRELATION-BASED METHOD FOR QUANTITATIVE IVUS BLOOD FLOW AT 20 MHz

FERMÍN A. LUPOTTI,*† AUDREY ZIMMER,‡ MICHEL DARONAT,‡ F. STUART FOSTER,§ ANTONIUS F. W. VAN DER STEEN*†[1] and GUY CLOUTIER‡

*Experimental Echocardiography, Thoraxcenter, Erasmus Medical Center, Rotterdam, The Netherlands; †Interuniversity Cardiology Institute of the Netherlands (I.C.I.N.), Utrecht, The Netherlands; ‡Laboratory of Biorheology and Medical Ultrasonics (L.B.U.M.), University of Montreal Hospital, Notre-Dame Hospital and Laboratory of Biomedical Engineering, Clinical Research Institute of Montreal (I.R.C.M.), Montreal, QUE, Canada; and §Sunnybrook & Women's College Health Science Center, Imaging/Bioengineering Research Center, Toronto, ONT, Canada

(*Received* 14 *November* 2002; *in final form* 9 *October* 2003)

Abstract—Recent computer simulations suggest that the presence of aggregates of red blood cells (RBCs), at random angles and lengths, does not affect the measurements of blood flow transverse to the ultrasound (US) beam direction using a correlation-based method and an intravascular (IV) US array catheter. However, in case of aggregates of RBCs aligned with the flow, measurements of simulated blood velocity are affected. Blood velocity gradients were also shown not to influence the correlation-based method for blood velocity estimation. The objective of this study was to quantify the influence of aggregates of RBCs and blood velocity gradients on the correlation-based method during *in vitro* experiments. For this purpose, measurements were performed on washed RBCs (no aggregation), normal human blood, and two types of diseased blood in which a lower or a higher level of aggregation was present. The decorrelation pattern of a circular US transducer as a function of transverse blood flow was studied using a Couette system. Changing the shear rate of the Couette system modified the aggregation level of RBCs and the velocity gradient. With the exception of the results at low shear rates and abnormally high aggregation levels, agreements were found between the autoconvolution of the acoustical beam (reference curve) and the radiofrequency (RF) decorrelation patterns. For the high shear rate present in coronary arteries, the correlation-based method for blood flow estimation should not be influenced by these phenomena. (E-mail: a.vandersteen@erasmusmc.nl)

Key Words: **Intravascular ultrasound, Ultrasound beam, Couette system, Shear rate, Aggregation of RBCs, Transverse blood flow, Decorrelation patterns.**

INTRODUCTION

Intravascular ultrasound (IVUS) imaging has become a valuable diagnostic tool in interventional cardiology (Saijo and van der Steen 2003). Radiofrequency (RF) data processing has significantly enhanced the potential of IVUS (van der Steen et al. 1998). In addition, IVUS has been applied to measure blood flow velocity and volumetric flow (Li et al. 1998). Decorrelation of the backscattered signal has proven to be proportional to the transverse blood velocity and is related to the characteristics of the acoustical beam.

When red blood cells (RBCs) flow through a vessel, they can form aggregates known as rouleaux (Chien 1974; Fung 1993). Depending on the characteristics of the blood sample and flow rate, complex 3-D networks also can be formed. RBC aggregation has been associated with diabetes (Le Devehat et al. 1990), dyslipidemia (Razavian et al. 1992), hypertension (Zannad et al. 1988), cardiac and cerebral vascular diseases (Neumann et al. 1991), thromboembolic events (Chabanel et al. 1994), carcinoma and inflammation (Weng et al. 1996). RBC aggregation depends basically on three conditions:

[1] Antonius F. W. van der Steen is the 2000 NWO PIONIER Technical Sciences.

Address correspondence to: Dr. Antonius F. W. van der Steen, Erasmus University, Rotterdam, Room Ee 23.02, P.O. Box 1738, Rotterdam, 3000 DR The Netherlands. E-mail: a.vandersteen@erasmusmc.nl

a sufficient concentration of RBCs (*i.e.*, hematocrit), a sufficient concentration of macromolecules (*i.e.*, fibrinogen and others) and a shear rate in blood low enough to leave the aggregates intact (Chien 1974). When the shear rate increases ($> 100\ s^{-1}$), the aggregation of RBCs ceases to be important, and the blood cells tend to become elongated and aligned with the streamline of flow to reduce the blood viscosity (Fung 1993). Aggregation is a reversible process and, when the shear rate is lowered ($< 100\ s^{-1}$), the rouleaux can be formed again. Weng et al. (1996, 1998) studied the influence of acute-phase proteins (a group of plasma glycoproteins synthesized by the liver) on erythrocyte aggregation. The proteins such as haptoglobin (Hp), C-reactive protein (CRP) and ceruloplasmin (Cp) had an effect on the aggregation and adhesive forces between erythrocytes; more specifically, abnormally high levels of Hp and Cp induced a significant increase in the reversible erythrocyte rouleau formation, and CRP and Cp increased the adhesive forces of the aggregates. In patients with unstable angina pectoris, abnormal RBC aggregation levels were found to be predictive of subsequent acute myocardial infarction (Neumann et al. 1991).

During human IVUS interventions, the US transducer is in direct contact with blood; the US beam is not attenuated or deflected by any other structure, such as tissue. Van der Heiden et al. (1995) showed that, for a rotating single-element IVUS catheter with a central frequency of 30 MHz, when RBC aggregation goes on during blood flow, the integrated backscatter power increases. Recently, Lupotti et al. (2000, 2001) studied the decorrelation characteristics of an IVUS array catheter during transverse blood flow. First, blood was simulated as a collection of omnidirectional and randomly located point scatterers as single RBCs and, second, strings of point scatterers at random angles and lengths as normal physiologic aggregates of RBCs simulated blood in a more general way. Agreements were found between decorrelation patterns from both scattering media and the autoconvolution of the acoustical beam used as a reference curve. The autoconvolution of the acoustical beam is defined as the convolution of the measured line spread function at a given depth with itself (reference curve A_{2D} in Appendix A in Lupotti et al. 2000). However, when the strings of point scatterers were aligned with the flow, the rate of decorrelation became lower. Simulation of blood flow with a linear blood-velocity gradient or shear rate (*e.g.*, near the vessel boundaries for parabolic blood flow) was performed, but produced no effect on the mean decorrelation pattern (Lupotti et al. 2002c). In that last study, point scatterers were considered and the possible effect of rouleaux was ignored.

In the present study, *in vitro* experiments were performed to corroborate previous simulation studies on the influence of aggregates of RBCs and linear blood-velocity gradients on the correlation-based method for blood velocity estimation. The decorrelation pattern of the RF signals caused by transverse blood flow was studied using a circular US transducer in a Couette system. Because previous studies showed the decorrelation pattern from blood flow in agreement with the autoconvolution of the acoustical beam, the latter curve will be used as a reference curve during the present study. Whole human blood samples drawn from healthy volunteers and from patients were used. The Couette system produces a stable linear velocity gradient or shear rate that, when varied, modifies the level of aggregation of RBCs in the whole blood. The objective of this study was to quantify the influence of aggregates of RBCs and linear blood-velocity gradients on the correlation-based method during transverse blood flow, and judge how this could affect the measurements of blood velocity.

MATERIALS AND METHODS

Blood samples

Whole blood was freshly drawn from 20 individuals and immediately anticoaugulated with ethylenediamine tetra acetic acid (EDTA, 3 g/L); 8 blood samples were from healthy volunteers from our institutional staff, 2 were from a blood bank, and 10 were from patients with a disease that could increase the aggregation of RBCs, such as cardiovascular disease, diabetes, hypercholesterolemia, hypertension, hyperlipidemia, thrombosis or heavy smoking. The hematocrit of the donor was not adjusted and, thus, remained at its physiologic value for the 8 normal and 10 diseased blood samples. The blood samples of patients collected during peripheral interventions represent a typical population normally prescribed for an IVUS examination of their coronary arteries. The two larger blood volumes, obtained from the blood bank, were used to produce washed blood samples where the hematocrit was set as close as possible to 40%. These two blood samples were centrifuged and the plasma was replaced with a saline solution; this washing procedure was repeated 3 times to remove any plasma proteins promoting aggregation. The three groups of sample blood are identified here as normal blood, diseased blood and washed RBCs, respectively. The diseased blood samples were subdivided into two subgroups according to the aggregation level measured with an erythroaggregameter.

Blood tests

Blood tests, such as the hematocrit and the aggregation level, were performed on all blood samples used in this study. The hematocrit was measured using a microcentrifuge system (Haemofuge, Heraeus Sepatech

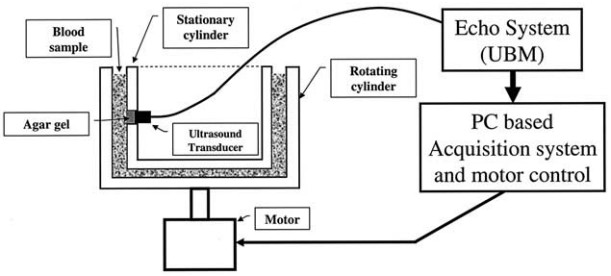

Fig. 1. Experimental setup; the Couette system formed by two cylinders. The outer cylinder rotates at a given angular velocity driven by the motor; the inner one is fixed and holds the US transducer. The blood sample (≈ 50 mL) flows in the 2-mm gap between the coaxial cylinders.

GmbH, Osterode/Harz, Germany) at 12000 rpm for 10 min. The RBC aggregation level was determined with an erythroaggregameter based on a Couette flow arrangement (Regulest, Florange, France) (Houbouyan et al. 1997). A blood volume of 1.5 mL was needed to perform these measurements. The instrument provides information on the aggregation time (s), the mean kinetic index at 10 s or aggregation index (S_{10}, no unit), partial (γ_D s^{-1}) and total dissociation thresholds (γ_S s^{-1}). The aggregation time was obtained from the inverse of the slope of the scattered light intensity variation between 0.3 and 1.9 s after stoppage of the flow rotation. The index S_{10} was calculated as the ratio of the area above the light intensity curve during the first 10 s following flow stoppage to the total area within the same period of time. The partial dissociation threshold (γ_D) was obtained from the intersection of a regression line computed for shear rates below 20 s^{-1} and a horizontal line intercepting the maximum of the scattered light intensity, and the total dissociation threshold (γ_S) corresponded to the shear rate at the maximum scattered light intensity. These last two parameters provide information about the adhesive forces between RBCs. Low values of S_{10}, γ_D and γ_S indicate a low level of aggregation and *vice versa* (Cloutier and Qin 2000).

Experimental setup

The experimental setup was comprised of a Couette system, an echo system (VS40 Ultrasound BioMicroscope (UBM), VisualSonics Inc., Toronto, ON, Canada) and a PC-based acquisition system (Fig. 1).

The Couette system. The Couette system was used to produce linear blood velocity gradient profiles at a given shear rate (Whorlow 1980; van der Heiden et al. 1995). It requires only 50 mL of blood. The system consists of a stationary inner cylinder and a rotating outer cylinder (Fig. 1). The gap between cylinders was 2 mm, where the blood shear rate is constant. The Couette flow system of the current study was originally designed for US high-frequency blood backscattering measurements (Foster et al. 1994).

The ultrasound transducer and the echo system. The US transducer, a 36-MHz focused 3-mm circular PVDF transducer (−6 dB band width of 18 to 54 MHz focused at 6 mm), was excited at a pulse-repetition frequency (PRF) of 5 kHz. The transducer was placed in the stationary inner cylinder (Fig. 1). The positioning of the transducer, perpendicular to the area of interest and at the right focal length, was important for obtaining the best RF signals for measuring the decorrelation patterns. The transducer was screwed within the inner cylinder made of Plexiglas. Agar gel was used to fill the acoustic window between the transducer surface and the blood sample. The UBM echo system provides controls of the gain, filters and central frequency that were adjusted to optimize the signal-to-noise ratio (SNR). The US system fired bipolar square wave pulses at a central frequency of 19 MHz, the UBM band-pass filter was set to 10 to 80 MHz, and a receiving gain around 23 dB was used for all the experiments. The window length for correlation coefficient estimation was 2 mm (gap between cylinders).

The PC-based acquisition system. The acquisition system was based on a PC with an acquisition board (CS 8500 GageScope board, Gage Applied Sciences Inc., Montreal, QUE, Canada) and the Compuscope software that allows the acquisition of multiple sets of RF signals. RF data were digitized at a sampling frequency of 250 MHz at 8 bits resolution; sets of RF signals at the PRF of 5 kHz were acquired with a time interval of 5 s between each set; this was performed for each shear rate to reach the steady-state plateau of aggregation. A computer program implemented in LabView (National Instruments, Austin, TX) was used to control the rotational speed (*i.e.*, the shear rate) of the outer cylinder of the Couette system.

Protocol for the experiments

All experiments were performed at room temperature (≈20°C). Before each experiment, the blood hematocrit and aggregation level were measured, as mentioned above. After the blood sample was placed in the Couette system, the measurements were performed as follows.

In the first 120 s, a shear rate of 600 s^{-1} was applied to break RBC aggregates. The shear rate was then reduced to values of 1, 5, 20, 40 or 80 s^{-1} and acquisition was performed for 140 s. The measurements were repeated twice for each blood sample and shear rate. A total of 36 sets of 120, 90 and 60 RF signals were acquired for shear rates of 1, 5 and 20 s^{-1}, respectively;

Table 1. Values, as mean ± SD, for the age, hematocrit, aggregation time, aggregation index S_{10} and the partial (γ_D) and total dissociation threshold (γ_S), from the normal, washed RBCs, and diseased blood samples Lag and Hag

Blood type	Age (years)	Hematocrit (%)	Aggregation time (s)	S_{10} (no unit)	γ_D (s^{-1})	γ_S (s^{-1})
Normal	26.1 ± 2.5	41.8 ± 2.6	3.7 ± 0.6	17.9 ± 2.0	40.9 ± 7.4	117 ± 21
Washed RBCs	not known	38.5 ± 0.7	1410 ± 1668	0.43 ± 0.02	17.7 ± 2.2	20.0 ± 2.8
Disease Lag	60.4 ± 11.1*	33.0 ± 3.2*	5.6 ± 2.0*	13.3 ± 3.3*	56 ± 25*	239 ± 148*
Disease Hag	69.8 ± 9.5*†	35.0 ± 2.3*†	2.87 ± 0.56*†	20.7 ± 2.7*†	82 ± 43*†	275 ± 92*‡

* $p < 0.0001$ (*t*-test); normal blood group vs. combined diseased blood groups; † $p < 0.005$ (*t*-test); diseased blood Lag vs. Hag; ‡ $p = 0.023$ (*t*-test); diseased blood Lag vs. Hag.

and 36 sets of 30 RF signals were acquired for shear rates of 40 and 80 s^{-1}. One set of RF signals, from the 36 sets, was acquired during the disaggregation phase just before the beginning of the aggregation phase, which is considered to be acquired at time 0.

Signal processing

Relative backscattered power. The relative backscattered signal power (in dB) as a function of time was calculated to follow the aggregation of the RBCs. Because all measurements were performed at the same distance from the transducer using the same window length as a setting of the system, no correction was made for the beam characteristics of the transducer for the assessment of the backscattered power. The relative backscattered signal power is defined as 10 times the base 10 logarithm of the summation of the squared backscattered RF signal components normalized by the number of sample points. The mean rising slopes of the backscattered power as a function of time was calculated (in dB/s) based on measurements at time 0 and at 20 s in the aggregation phase.

Statistical analysis. The correlation coefficient $\rho_{i,j}$ between two RF signals, s_i and s_j, was calculated using a standard method as described by Lupotti et al. (2000). The backscattered signal from blood (about 2 mm in length) was used for the calculation of the correlation coefficients. The sets of RF signals acquired after 60 s of the aggregation phase (*i.e.*, at the plateau of the aggregation process) were used for the calculation of the decorrelation patterns. Because the correlation coefficients are not normally distributed, the Fisher *Z* transform was used to present the results (Fisher 1970; Lupotti et al. 2000).

Noise correction method

To estimate and suppress the decorrelation due to noise from the total decorrelation, a method introduced by Lupotti et al. (2002b) was used during this study. Briefly, the method uses the fact that the decorrelation pattern should be 1 at lag zero; however, this does not occur in the presence of noise in the RF signals. Noise produces an offset in the decorrelation pattern by shifting the decorrelation pattern down and, thus, the correlation coefficient at lag zero may not be unity (the second figure in Lupotti et al. 2002b). The correlation coefficient at lag zero is then estimated by curve fitting of the estimated correlation coefficients. Because the entire decorrelation pattern was studied, all correlation coefficients were normalized by the correlation coefficient at lag zero to correct them for noise.

Acoustical beam

The acoustical beam of the transducer was measured to calculate its autoconvolution, which is used as a reference curve; the device used for the measurements was previously described by Lupotti et al. (2002a). Briefly, a line target is moved transversely across the US beam at the depth of interest; then the autoconvolution of the measured acoustical beam is performed and normalized by the maximum. The mean autoconvolution of the measured US beam is based on measurements performed at 5.5, 6 and 6.5 mm from the transducer.

Outline of the results

Considering the fact that some patients were under medication, the patient's group was subdivided into two subgroups, the low (Lag) and high aggregation level (Hag) groups. The parameter used to discriminate between groups was the aggregation time measured with the erythroaggregameter. As shown next, the relative backscattered signal power is plotted as a function of time for the normal and diseased blood samples. Results for relative backscattered signal power with the washed RBCs are not presented since no increase in the relative backscattered signal power was observed due to any cell aggregation as results of the washing procedure. The decorrelation patterns for all experiments are presented and compared with the autoconvolution of the acoustical beam, which is considered the reference curve.

RESULTS

Means and SDs of the physiologic parameters such as age (years), hematocrit (%), aggregation time (s),

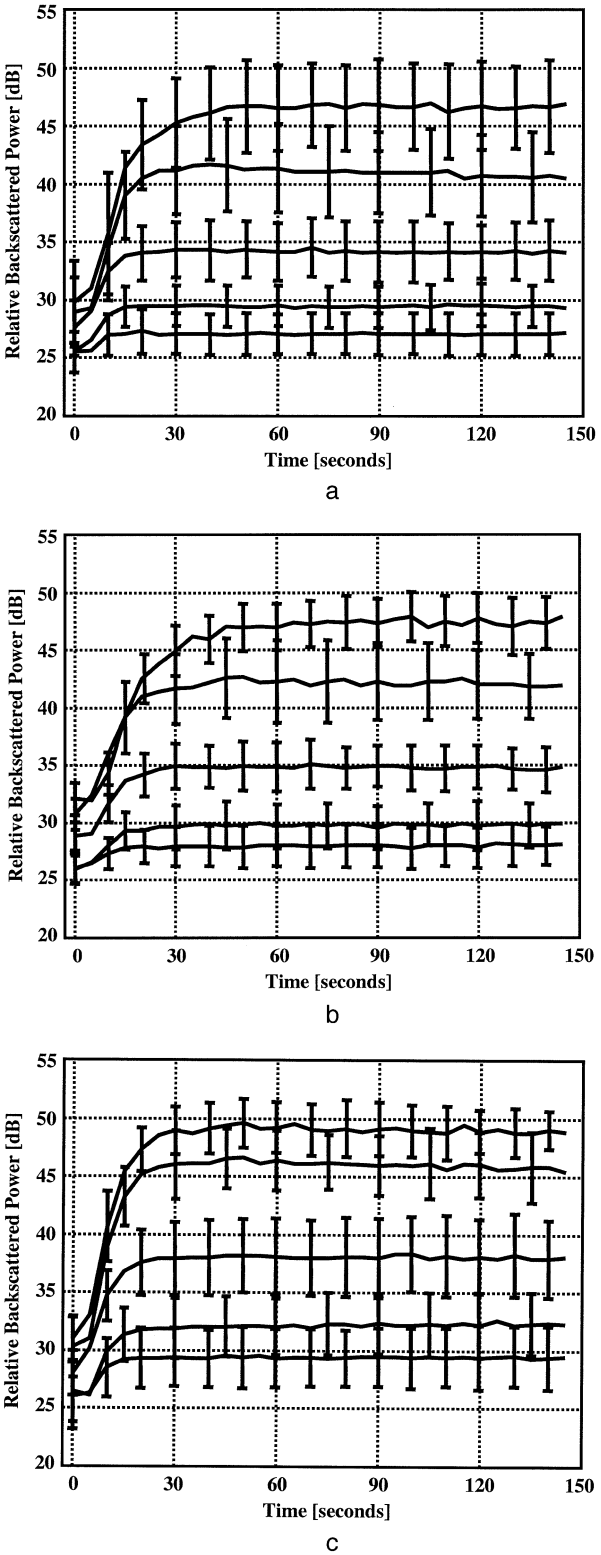

Fig. 2. Means and SDs for the relative backscattered signal power (in dB) as a function of time for shear rates of 1, 5, 20, 40 and 80 s^{-1}, from top to bottom, respectively; (a) for normal blood, (b) for diseased blood Lag, and (c) for diseased blood Hag.

Table 2. Mean rising slope values of the aggregation process measured from time 0 to 20 s for normal, Lag and Hag blood samples

Shear rate (s^{-1})	Normal (dB/s)	Lag (dB/s)	Hag (dB/s)
1	0.67	0.52	0.81
5	0.57	0.51	0.74
20	0.32	0.26	0.48
40	0.19	0.16	0.26
80	0.09	0.09	0.16

aggregation index S_{10} (no unit), and partial (γ_D, in s^{-1}) and total dissociation thresholds (γ_S, in s^{-1}) are presented in Table 1. Highly significant differences for the hematocrit were observed between normal blood and the combined diseased blood groups for all parameters as well as diseased blood groups. The aggregation time for diseased blood Lag was higher than that from normal blood; however, lower values for S_{10}, γ_D and γ_S were found for the Lag group compared to those from the Hag group. Figure 2 shows the relative backscattered signal power (in dB) as a function of time for shear rates of 1, 5, 20, 40 and 80 s^{-1}, from the top to the bottom, respectively, for normal (Fig. 2a) and for diseased blood Lag (Fig. 2b) and Hag (Fig. 2c). The aggregation of RBCs becomes faster for diseased blood samples, mainly for the group Hag, as expected by the low aggregation time and high indexes such as S_{10}, γ_D and γ_S. Table 2 presents the values of the mean rising slopes of the aggregation of RBCs process for normal, Lag and Hag blood samples.

Figure 3 shows the measured mean decorrelation pattern and SDs as a function of transverse displacements, as well as the mean autoconvolution of the acoustical beam, for (a) 1 and 5 s^{-1} and (b) 20, 40 and 80 s^{-1} for washed RBCs. Similar results are presented in Figs. 4, 5 and 6 for normal blood, Lag and Hag groups, respectively. Decorrelation patterns are compared with the autoconvolution of the acoustical beam used as a reference curve. Close agreements between mean decorrelation patterns and the autoconvolution of the acoustical beam for all blood samples and shear rates are observed, except for the Hag blood samples, where the decorrelation patterns for low shear rates (1 and 5 s^{-1}) are slower than the expected theoretical values.

DISCUSSION

From the parameters presented in Table 1, a difference on the hematocrit and age between groups was found that could influence the aggregation level. For the diseased groups Lag and Hag, the hematocrit is lower than for that from normal blood; a slight difference is also observed

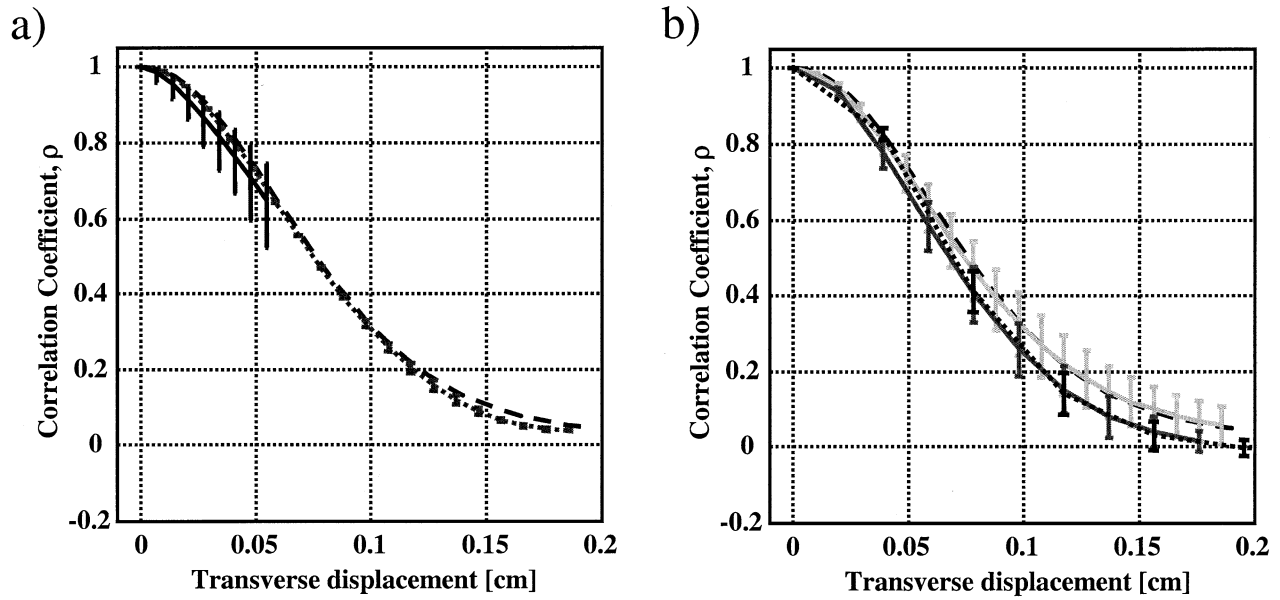

Fig. 3. Mean decorrelation pattern and SDs as a function of transverse displacements for washed RBCs at shear rates of (a) 1 (—) and 5 (· · · ·) s^{-1}, and (b) 20 (light grey line), 40 (dark gray line) and 80 (· · · ·) s^{-1}, in comparison with the autoconvolution of the acoustical beam (----).

between hematocrits from Lag and Hag. Other research groups already studied the influence of the hematocrit on the aggregation of RBCs. Kitamura et al. (1995) showed for three hematocrit levels (20%, 40% and 60%) and a constant level of fibrinogen, an effective scatterer diameter of approximately 70 μm was reached; the effective scatterer

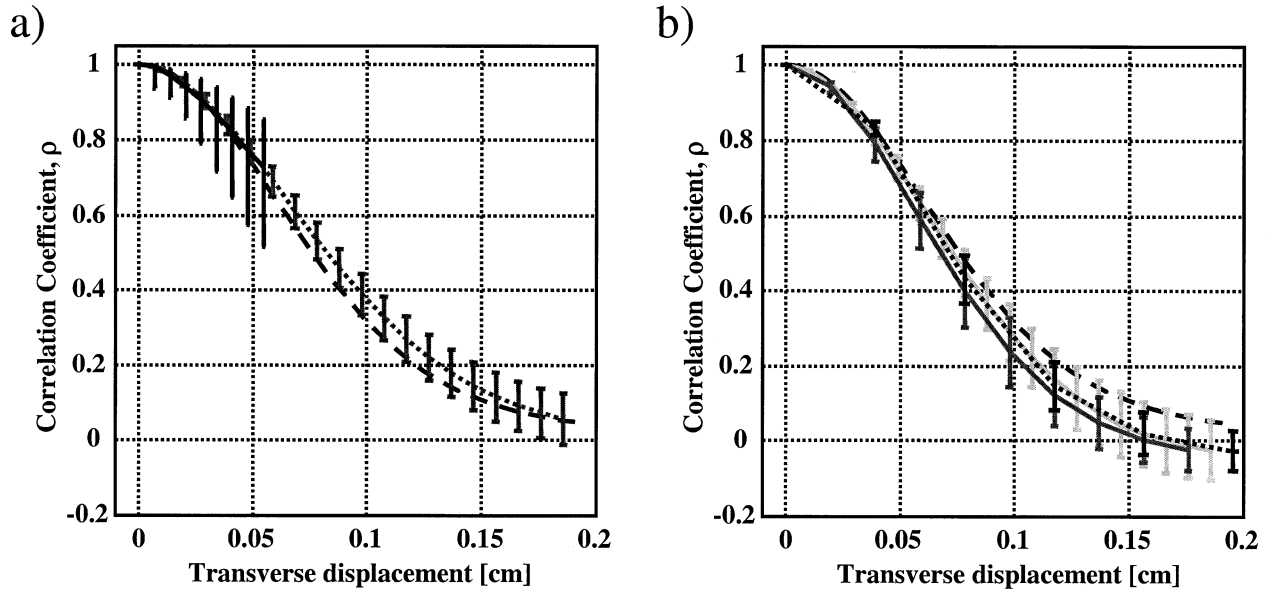

Fig. 4. Mean decorrelation pattern and SDs as a function of transverse displacements for normal blood samples at shear rates of (a) 1 (—) and 5 (dotted dark gray line) s^{-1}, and (b) 20 (light gray line), 40 (dark gray line) and 80 (· · · ·) s^{-1}, in comparison with the autoconvolution of the acoustical beam (----).

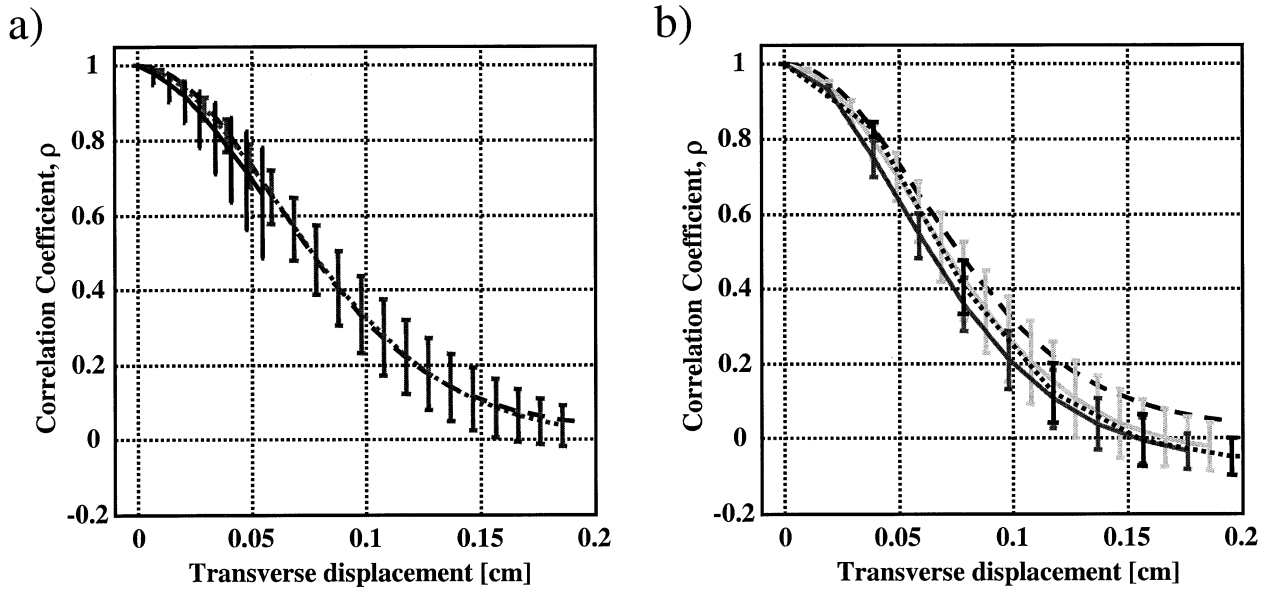

Fig. 5. Mean decorrelation pattern and SDs as a function of transverse displacements for diseased blood Lag at shear rates of (a) 1 (—) and 5 (dotted dark gray line) s^{-1}, and (b) 20 (light gray line), 40 (dark gray line) and 80 (· · · ·) s^{-1}, in comparison with the autoconvolution of the acoustical beam (----).

diameter was measured by using the power spectrum computed as the squared magnitude of the Fast Fourier transform of the windowed signal.

However, the rate at which this occurred varied with the hematocrit; a lower rate of aggregation for the low hematocrit was found. This could explain the higher aggre-

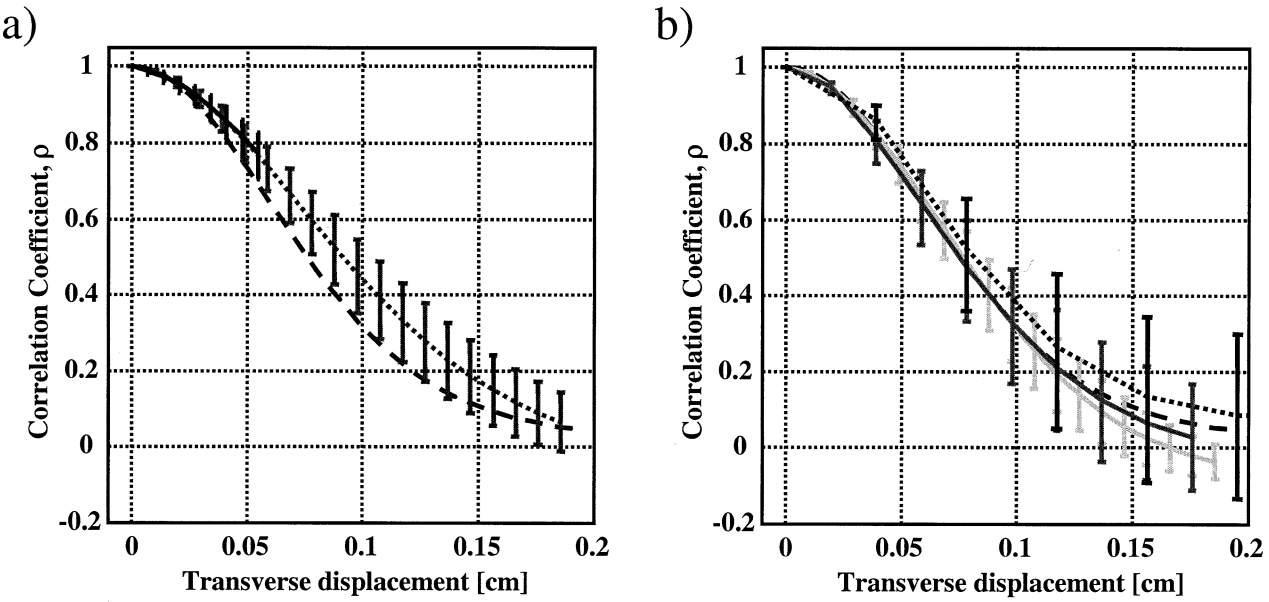

Fig. 6. Mean decorrelation pattern and SDs as a function of transverse displacements for diseased blood Hag at shear rates of (a) 1 (—) and 5 (dotted dark gray line) s^{-1}, and (b) 20 (light gray line), 40 (dark gray line) and 80 (· · · ·) s^{-1}, in comparison with the autoconvolution of the acoustical beam (----).

gation time for disease blood Lag compared to Hag. Regarding the mean age of the groups of blood samples, Linderkamp et al. (1984) studied the RBC aggregation in preterm and term neonates and adults by means of a rheoscope (increase in light transmission during blood stasis). Both the rate and extent of RBC aggregation were low in the premature infants, increased with gestational age, and reached the highest values in the adults. Based on that study and because, for the present study, all blood samples were drawn from adult volunteers and patients, no influence in the aggregation level due to difference in age can be expected. During the present study, the *in vitro* measurements were performed at room temperature (≈20°C) and not at the physiologic temperature of 37°C, which could affect the process of formation and size of aggregates of RBCs. Neumann et al. (1987) studied the effect of temperature on the level of aggregation of RBCs at 3, 10, 20, 30 and 37°C from normal donors and blood samples of patients with venous ulcers of the leg. Although red cell aggregate formation as an overall process is retarded by a decrease in temperature and the aggregates become more resistant to hydrodynamic dispersion, they become more prone to growing under low shear stress. Neumann and colleagues concluded that, as a whole, red cell aggregation is favored by temperature lowering.

The results presented in Fig. 2 showed an increase in the mean rising slope of the aggregation process from the normal and diseased blood Lag to the Hag group for all shear rates (Table 2), which corresponds with the shorter aggregation time (measured by the erythroaggregameter) from diseased blood sample Hag (Table 1). The relative backscattered signal power from diseased blood Hag is higher than other blood samples for all shear rates, which suggests larger formation of aggregates of RBCs. This is also expected from the high indexes S_{10}, γ_D and γ_S from this group. During the disaggregation phase (high shear rate, 600 s^{-1}), red cell aggregation is expected to fully cease and, thus, similar relative backscattered signal power should be observed.

The results presented in Fig. 3 for washed RBCs suggest that a linear velocity gradient does not affect the measurements of blood velocity using a correlation-based method, even when a large window size (2 mm in this case) is used for the calculations, which includes a large range of blood velocities. Nevertheless, most blood velocity estimator methods use a window length of about a wavelength. For IVUS blood flow measurements, at a central frequency from 20 MHz, the wavelength is about 0.075 mm, which covers a small range of blood velocities. Consequently, the current study may be conservative and the broad range of velocities within the region of interest may explain the tendency toward a faster decorrelation than expected at the higher shear rates of 20, 40 and 80 s^{-1}. For quantitative IVUS blood flow measurements using a correlation-based method, correlation values ranging from 1 to 0.5 are normally used. Correlation coefficients lower than 0.5 means an SNR below 0 dB (Céspedes et al. 1997); for such transverse displacements, the scatterers remain for a short period of time within the US sample volume, which produces a large decorrelation between RF signals.

Generally, close agreements between the mean decorrelation pattern and the theoretical values were observed at all shear rates, for the normal and diseased blood groups (Figs. 4, 5 and 6), except at shear rates of 1 and 5 s^{-1} for Hag blood samples. The lower rate of decorrelation may be explained by the size and orientation of the aggregates of RBCs, as described by the theoretical study of Lupotti et al. (2001). When the scattering medium resembles a unidirectional medium, the rate of decorrelation tended to be closer to 1 for small displacements. In a Couette system, because both cylinders are concentric, aggregates of RBCs could aligned with the flow (Chien et al. 1970), which causes the RF signals to remain correlated for longer periods of time as observed by the decorrelation patterns for the Hag blood sample at these very low shear rates (1 and 5 s^{-1}) (Fig. 6).

The high indexes S_{10}, γ_D and γ_S, aggregation index, partial and total dissociation threshold, respectively, from diseased blood Hag indicate the formation of large aggregates of RBCs. The SDs of the measurements increases from the washed RBCs to diseased blood samples. Aggregates of RBCs are large structures that are coming in and out of the acoustical beam introducing large changes in the RF signals, which contributes to an increase of the SDs of the decorrelation patterns. The fact that the US transducer must be removed and cleaned after each experiment may introduce some variations between experiments, also.

In clinical practice, interventional cardiologists are most interested in blood flow through coronary arteries, which are usually curved; the conditions for laminar flow are, in these arteries, hardly ever reached. The presence of an IVUS catheter inside the lumen of an artery also disturbs the blood flow profile. All phenomena that disturb the velocity profile (*e.g.*, shear rate > 100 s^{-1}) will result in a reduction of the RBC aggregate formation (van der Heiden et al. 1995). He and Ku (1996) studied the pulsatile flow in the human left coronary artery bifurcation, by a numerical study, for realistic *in vivo* anatomic and physiological conditions. It was shown that the mean wall shear stress during an entire cardiac cycle at the root and downstream of the left coronary artery is around 20 dyn/cm^2 (≈ 2 Pa). This indicates that, for a non-Newtonian fluid where the viscosity at infinity (shear rates > 100 s^{-1}) is 3.5 cP, the mean wall shear rate is around 570 s^{-1}. Similar results were found by Lee et al. (2001) for coronary and aortic circulation. A mean wall shear stress of 19.84 dyn/cm^2 was obtained through

a numerical analysis based on *in vivo* hemodynamic parameters. A shear rate close to 0 s^{-1} is expected at the center of the vessel and, thus, a mean shear rate across the vessel can be estimated as being around 250 s^{-1}.

Blood flow pulsatility, highly present in coronary arteries, produces changes in the shear rate across the vessel lumen as a function of the timing within the cardiac cycle (Milnor 1989). The velocity profile is flat during early systole (*i.e.*, low shear rates), becomes almost parabolic at peak systole (depending on the hematocrit) (*i.e.*, high shear rates), and then flattens again during diastole. Using a 30-MHz IVUS catheter, De Kroon et al. (1991) measured a cyclic variation of the backscattered power at 70 beats/min in the Iliac artery of three patients, which suggests that, at higher frequency, dynamic changes in aggregate size between systole and diastole can be observed. However, Cloutier and Shung (1993) suggested that a prolonged diastole is necessary to observe, at 10 MHz, an aggregate size enlargement in systole, because no cyclic variation on the Doppler power was found during pulsatile flow at 70 beats/min by using whole porcine blood. Rouleau formation, during systole and at 70 beats/min, was not observed probably because the red cells do not have enough time in diastole to be brought into contact and to align themselves. Because flow accelerates with a flat and more parabolic profile in late systole, the aligned red cells then probably form rouleaux until the shear rate becomes sufficient to break them totally or partially.

CONCLUSIONS

In this paper, the influence of the aggregation of RBCs and of linear velocity gradients on the correlation-based method for blood velocity estimation was assessed. Whole human blood and a Couette system were used for this purpose. The decorrelation patterns were not affected by linear velocity gradients when washed RBCs were used. Aggregation of RBCs showed no effect on the decorrelation patterns, except at very low shear rates and for highly aggregating blood (*i.e.*, large aggregates of RBCs). Overall, for the high shear rate present in coronary arteries, the correlation-based method for blood flow estimation should not be influenced by these phenomena when a small window length is used for the evaluations. However, the impact of the US frequency selected and that of dynamic changes in aggregate sizes as a function of time are factors that may need additional consideration because their effects on the decorrelation patterns have not yet been studied.

Acknowledgments—The authors acknowledge Dr. Gilles Soulez from the Interventional Radiologist Department of Radiology, University of Montreal Hospital (Notre-Dame Hospital), for providing the blood samples of patients with peripheral vascular disease. This work was supported by the Institutes of Health Research of Canada (#MOP-36467) and by the Fonds de la Recherche en Santé du Québec.

REFERENCES

Céspedes EI, Ophir J, Alam SK. The combined effect of signal decorrelation and random noise on the variance of time delay estimation. IEEE Trans Ultrason Ferroelec Freq Control 1997;44(1):220–225.

Chabanel A, Horellou MH, Conard J, Samama MM. Red blood cell aggregability in patients with a history of leg vein thrombosis: Influence of post-thrombotic treatment. Br J Haematol 1994;88(1): 174–179.

Chien S. Biophysical behavior of red cells in suspensions. In: Surgenor DM, ed. The red blood cell. San Francisco: Academic Press, 1974:1021–1133.

Chien S, Usami S, Dellenback RJ, Gregersen MI. Shear-dependent interaction of plasma proteins with erythrocytes in blood rheology. Am J Physiol 1970;219(1):143–153.

Cloutier G, Qin Z. Shear rate dependence of ultrasound backscattering from blood samples characterized by different levels of erythrocyte aggregation. Ann Biomed Eng 2000;28:399–407.

Cloutier G, Shung KK. Study of red cell aggregation in pulsatile flow from ultrasonic Doppler power measurements. Biorheology 1993; 30:443–461.

de Kroon MGM, Slager CJ, Gussenhoven WJ, et al. Cyclic changes of blood echogenicity in high-frequency ultrasound. Ultrasound Med Biol 1991;17:723–728.

Fisher RA. Statistical methods for research workers. Einburgh, UK: Oliver and Boyd, 1970.

Foster FS, Ohara H, Bloomfield T, Ryan LK, Lockwood G. Ultrasound backscatter from blood in the 30 to 70 MHz frequency range. IEEE Ultrason Sympos, 1994;3:1599–1602.

Fung YC. The flow properties of blood. Biomechanics: Mechanical properties of living tissues. New York: Springer-Verlag, 1993.

He X, Ku DN. Pulsatile flow in the human left coronary artery bifurcation: Average conditions. J Biomech Eng 1996;118(1):74–82.

Houbouyan LL, Delamaire M, Beauchet A, et al. Multicenter study of an erythro-aggregometer: Quality control and standardization. Clin Hemorheol 1997;17:299–306.

Kitamura H, Sigel B, Machi J, et al. Roles of hematocrit and fibrinogen in red cell aggregation determined by ultrasonic scattering properties. Ultrasound Med Biol 1995;21:827–832.

Le Devehat C, Vimeux M, Bondoux G, Khodabandehlou T. Red blood cell aggregation in diabetes mellitus. Int Angiol 1990;9(1):11–15.

Lee BK, Kwon HM, Hong BK, et al. Hemodynamic effects on atherosclerosis-prone coronary artery: Wall shear stress/rate distribution and impedance phase angle in coronary and aortic circulation. Yonsei Med J 2001;42(4):375–383.

Li W, van der Steen AFW, Lancée CT, Céspedes EI, Bom N. Blood flow imaging and volume flow quantitation with intravascular ultrasound. Ultrasound Med Biol 1998;24(2):203–214.

Linderkamp O, Ozanne P, Wu PY, Meiselman HJ. Red blood cell aggregation in preterm and term neonates and adults. Pediatr Res 1984;18(12):1356–1360.

Lupotti FA, Céspedes EI, Mastik F, van der Steen AFW. IV US flow measurements: Line spread function and decorrelation pattern. Ultrasonics 2002a;40:843–847.

Lupotti FA, Céspedes EI, van der Steen AFW. Decorrelation characteristics of transverse blood flow along an intravascular array catheter. IEEE Trans Ultrason Ferroelec Freq Control 2000;47(6):1582–1592.

Lupotti FA, Céspedes EI, van der Steen AFW. Decorrelation characteristics of transverse blood flow along an intravascular array catheter: Effects of aggregation of red blood cells. Ultrasound Med Biol 2001;27(3):409–417.

Lupotti FA, de Korte CL, Mastik F, van der Steen AFW. Dynamic noise correction for IV US quantitative volume blood flow: Methods and numerical validation. Ultrasound Med Biol 2002b;28(8):1053–1060.

Lupotti FA, van der Steen AFW, Mastik F, de Korte CL. Decorrelation-based blood flow velocity estimation: Spread of flow velocity,

linear flow velocity gradients and parabolic flow. IEEE Trans Ultrason Ferroeled Freq Control 2002c;49(6):705–714.
Milnor WR. Hemodynamics. Baltimore, MD: Waverly Press, 1989.
Neumann FJ, Katus HA, Hoberg E, et al. Increased plasma viscosity and erythrocyte aggregation: Indicators of an unfavourable clinical outcome in patients with unstable angina pectoris. Br Heart J 1991;66:425–430.
Neumann FJ, Schmid-Schonbein H, Ohlenbusch H. Temperature-dependence of red cell aggregation. Pflugers Arch Eur J Physiol 1987;408(5):524–530.
Razavian SM, Del Pino M, Simon A, Levenson J. Increase in erythrocyte disaggregation shear stress in hypertension. Hypertension 1992;20(2):247–252.
Saijo Y and van der Steen AFW, eds. Vascular Ultrasound. Tokyo: Springer-Verlag, 2003.
van der Heiden MS, de Kroon MGM, Bom N, Borst C. Ultrasound backscatter at 30 MHz from human blood: Influence of rouleau size affected by blood modification and shear rate. Ultrasound Med Biol 1995;21(6):817–826.
van der Steen AFW, Céspedes EI, de Korte CL, et al. Novel developments in intravascular imaging. IEEE Ultrason Sympos 1998;2: 1733–1742.
Weng X, Cloutier G, Beaulieu R, Roederer GO. Influence of acute-phase proteins on erythrocyte aggregation. Am J Physiol 1996;271: H2346–H2352.
Weng X, Roederer GO, Beaulieu R, Cloutier G. Contribution of acute-phase proteins and cardiovascular risk factors to erythrocyte aggregation in normolipidemic and hyperlipidemic individuals. Thromb Haemost 1998;80:903–908.
Whorlow RW. Rotational viscometers. Chichester, UK: Ellis Horwood, 1980.
Zannad F, Voisin P, Brunotte F, et al. Haemorheological abnormalities in arterial hypertension and their relation to cardiac hypertrophy. J Hypertens 1988;6(4):293–297.